Applicability of the equations-of-motion technique for quantum dots

Vyacheslavs Kashcheyevs,[1,*] Amnon Aharony,[1,2] and Ora Entin-Wohlman[1,2,3]
[1]*School of Physics and Astronomy, Raymond and Beverly Sackler Faculty of Exact Sciences, Tel Aviv University, Tel Aviv 69978, Israel*
[2]*Department of Physics, Ben Gurion University, Beer Sheva 84105, Israel*
[3]*Albert Einstein Minerva Center for Theoretical Physics, Weizmann Institute of Science, Rehovot 76100, Israel*
(Received 28 November 2005; published 27 March 2006)

The equations-of-motion (EOM) hierarchy satisfied by the Green functions of a quantum dot embedded in an external mesoscopic network is considered within a high-order decoupling approximation scheme. Exact analytic solutions of the resulting coupled integral equations are presented in several limits. In particular, it is found that at the particle-hole symmetric point the EOM Green function is temperature independent due to a discontinuous change in the imaginary part of the interacting self-energy. However, this imaginary part obeys the Fermi liquid unitarity requirement away from this special point, at zero temperature. Results for the occupation numbers, the density of states, and the local spin susceptibility are compared with exact Fermi liquid relations and the Bethe ansatz solution. The approximation is found to be very accurate far from the Kondo regime. In contrast, the description of the Kondo effect is valid on a qualitative level only. In particular, we find that the Friedel sum-rule is considerably violated, up to 30%, and the spin susceptibility is underestimated. We show that the widely used simplified version of the EOM method, which does not account fully for the correlations on the network, fails to produce the Kondo correlations even qualitatively.

DOI: 10.1103/PhysRevB.73.125338 PACS number(s): 75.20.Hr, 72.15.Qm, 73.21.−b, 73.23.Hk

I. INTRODUCTION

Quantum dots embedded in mesoscopic structures are currently of great experimental and theoretical interest, because such systems allow for detailed and controlled studies of the effects of electronic correlations.[1] The theoretical description of these systems is usually based on the Anderson model,[2,3] in which the electronic correlations are confined to few impurities that represent the quantum dots. Although a rich variety of techniques has been developed over the years to treat the Anderson model,[4] their applications to the quantum dot systems are not straightforward. In such systems one would like to be able to study dynamical properties (e.g., transport) as function of the impurity characteristics (which can be tuned experimentally) over a wide range of parameters. This is not easily accomplished by the Bethe ansatz solution, for example.

The theoretical difficulty can be pinned down to the ability to derive a reliable, easy-to-handle, expression for the single-electron Green function on the quantum dot. Because the electronic interactions in the Anderson model take place solely on the dot, this Green function can be shown to determine, under certain conditions, the charge or the spin transmission through the quantum dot, the charge accumulated on it, etc.[3,5] Consequently, much effort has been devoted to finding faithful analytic approximations for this object. Alternative treatments rely on numerical techniques, such as quantum Monte Carlo,[6] or the numerical renormalization group (NRG) method.[7] NRG in particular is considered to be capable of providing accurate estimates of the Green function over a wide parameter range, although at the cost of running iterative diagonalizations for each parameter set, and a limited resolution at high energies and high magnetic fields.

A ubiquitous method to derive an analytical expression for the Green functions is to use the equations-of-motion (EOM).[8] In the case of the single-impurity Anderson model, the EOM of the (single-particle) impurity Green function gives rise to an infinite hierarchy of EOM of higher-order Green functions. A well-known approximation procedure is then to truncate this hierarchy, thus producing certain thermal averages representing various correlation functions. The latter need to be found self-consistently from the resulting closed set of equations. The level at which the EOM are truncated is chosen such that most of the interaction effects are captured.[9–12] This scheme has been applied to the original Anderson model a long time ago,[9–11,13,14] yielding approximate expressions for the resistivity,[9,10] the spin susceptibility,[10,13] and the magnetotransport[14] of dilute magnetic alloys. For temperatures above the Kondo temperature, T_K, these results agree with perturbation theory calculations.[4] Although several limitations of these self-consistent approaches are known (such as underestimation of the Kondo temperature or the absence of $(T/T_K)^2$ terms in the low-temperature expansion of the results), they still can form a basis for a qualitative analytic treatment of the Kondo effect.

The application of the EOM technique to a quantum dot system has been undertaken by Meir, Wingreen, and Lee[5] (MWL). Neglecting certain correlation functions, they have obtained a closed analytic expression for the dot Green function. Several subsequent studies have employed their scheme to describe various effects of the Kondo correlations in quantum dots in different settings, e.g., ac response of a biased quantum dot,[15] nonequilibrium Andreev tunneling,[16] and coupling to magnetic leads.[17] As we show below, the approximation of MWL fails in various aspects. Recent attempts to improve on that solution turned out to be not completely satisfactory: either requiring further approximations on top of the self-consistent truncation[18] or leading to iterative numerical solutions.[19–22] The truncation of the EOM at

an even higher order has been recently investigated numerically in Ref. 23. It is therefore of interest to examine whether an *exact solution* of the self-consistency equations of the EOM method will improve on the previous results, and will be capable of producing a reliable approximation for the Green function that can be used in the analysis of quantum dot systems.

In this paper we consider a quantum dot embedded in a general complex network, and obtain and solve the truncated EOM for its Green function. This EOM contains all the next-order correlation functions, which we decouple and calculate self-consistently. We first derive (in Sec. II) an integral equation for the Green function, allowing for arbitrary values of the on-site Coulomb interaction, U. We then analyze (in Sec. III) the properties of this EOM solution. We find that in the case of a particle-hole symmetric Hamiltonian the resulting Green function is *temperature independent* (a point which is overlooked in previous treatments of quantum dots, see for example Ref. 5). However, we show that this is a singular point in the parameter space. We also investigate the zero-temperature limit of the EOM solution, and show that it fails to satisfy the Friedel sum-rule. We then turn to the infinite U case (in Sec. IV), and derive an exact analytical solution to the integral equation for the Green function. In Sec. V we use this solution to obtain the total occupation number on the dot, and compare it with the exact solution supplied by the Bethe ansatz. This comparison shows that the EOM solution is faithful outside the Kondo regime, but fails in the regime where Kondo correlations play a dominant role. In particular, the Friedel sum-rule is violated by $\sim 30\%$, invalidating the assumptions made in previous studies.[11,19,21] We then derive the local spin susceptibility on the dot and demonstrate that the full self-consistent solution of the EOM, as used in this work, is required in order to obtain quantitatively correct results. We also examine the local density of states at the Fermi level, and find that it shows the expected universal behavior as function of T/T_K, though the EOM Kondo temperature lacks a factor of 2 in the exponential dependence on the single-energy level on the dot. Finally, we examine the EOM technique from another point of view (Sec. VI): We expand the Green function derived from the EOM to second order in the dot-network coupling, and compare the results with those obtained from a straightforward perturbation theory.[24,25] This comparison shows again the necessity to include in the EOM solution the full self-consistent calculation of all the correlations. A short summary in Sec. VII concludes the paper.

II. THE GREEN FUNCTION ON THE DOT

As mentioned above, several properties of the Anderson model can be expressed in terms of the Green function on the dot. Here we examine the determination of this function using the EOM method. Our discussion is limited to a single interacting impurity embedded in a general noninteracting network, for which the Hamiltonian can be written in the form

$$\mathcal{H} = \mathcal{H}_{\text{dot}} + \mathcal{H}_{\text{net}} + \mathcal{H}_{\text{net-dot}}. \tag{1}$$

Here, the dot Hamiltonian is given by

$$\mathcal{H}_{\text{dot}} = \sum_{\sigma} (\epsilon_0 + \sigma h) n_{d\sigma} + U n_{d\uparrow} n_{d\downarrow}, \quad n_{d\sigma} = d_{\sigma}^{\dagger} d_{\sigma}, \tag{2}$$

where $d_{\sigma}^{\dagger}$ (d_{σ}) is the creation (annihilation) operator of an electron of spin index $\sigma = \pm 1/2$ on the dot, ϵ_0 is the single-particle energy there, h is the Zeeman splitting, and U denotes the Coulomb repulsion energy. The noninteracting network is described by the tight-binding Hamiltonian

$$\mathcal{H}_{\text{net}} = \sum_{n\sigma} \varepsilon_{n\sigma} a_{n\sigma}^{\dagger} a_{n\sigma} - \sum_{mn\sigma} J_{mn} a_{m\sigma}^{\dagger} a_{n\sigma}, \tag{3}$$

where $a_{n\sigma}^{\dagger}$ ($a_{n\sigma}$) is the creation (annihilation) operator of an electron of spin index σ on the nth site on the network, whose on-site energy is $\varepsilon_{n\sigma}$, and $J_{mn} = J_{nm}^{*}$ are the hopping amplitudes on the network. Finally, the coupling between the dot and the network is given by

$$\mathcal{H}_{\text{net-dot}} = -\sum_{n\sigma} J_{n\sigma} d_{\sigma}^{\dagger} a_{n\sigma} + \text{H.c.} \tag{4}$$

We have allowed for spin-dependent on-site energies on the network, as well as spin-dependent hopping amplitudes between the dot and the network. In this way, our model includes also the case of spin-polarized leads connected to a quantum dot (see, for example, Refs. 5 and 21). The entire system is assumed to be at equilibrium with a reservoir held at temperature T (in energy units) and chemical potential $\mu = 0$.

Adopting the notations of Ref. 8, we write a general Green function in the form

$$\langle\langle A;B\rangle\rangle_{\omega \pm i\eta} \equiv \mp i \int_{-\infty}^{+\infty} \Theta(\pm t) \langle [A(t);B]_{+}\rangle e^{i(\omega \pm i\eta)t} dt, \tag{5}$$

where A and B are operators, Θ is the Heaviside function, and $\eta \to 0^{+}$. The Green function on the dot is then

$$G_{\sigma}(z) \equiv \langle\langle d_{\sigma}; d_{\sigma}^{\dagger}\rangle\rangle_{z}, \quad z \equiv \omega \pm i\eta. \tag{6}$$

In conjunction with the definition (5), a thermal average, $\langle BA\rangle$, is related to the corresponding Green function by

$$\langle BA\rangle = i \oint_{C} \frac{dz}{2\pi} f(z) \langle\langle A;B\rangle\rangle_{z}, \quad f(z) \equiv \frac{1}{1 + e^{z/T}}, \tag{7}$$

where the contour C runs clockwise around the real axis.

The EOM for the dot Green function is given in Appendix A [see Eq. (A2)]. As is shown there, that equation includes a higher-order Green function, whose EOM gives rise to additional Green functions. The resulting infinite hierarchy of EOM is then truncated according to a scheme proposed originally by Mattis[26] and subsequently used in Refs. 9–11, 13, 14, 18–21, and 27: Each Green function of the type $\langle\langle A^{\dagger}BC; d^{\dagger}\rangle\rangle$ in the EOM hierarchy is replaced by

$$\langle\langle A^{\dagger}BC; d^{\dagger}\rangle\rangle \Rightarrow \langle A^{\dagger}B\rangle \langle\langle C; d^{\dagger}\rangle\rangle - \langle A^{\dagger}C\rangle \langle\langle B; d^{\dagger}\rangle\rangle \tag{8}$$

if at least two of the operators A, B, and C are network operators $a_{n\sigma}$. Explicitly, the Green functions which are decoupled are $\langle\langle a_{n\sigma}d^{\dagger}_{\bar{\sigma}}a_{m\bar{\sigma}};d^{\dagger}_{\sigma}\rangle\rangle$, $\langle\langle a^{\dagger}_{n\bar{\sigma}}d_{\bar{\sigma}}a_{m\sigma};d^{\dagger}_{\sigma}\rangle\rangle$, and $\langle\langle a^{\dagger}_{n\bar{\sigma}}a_{m\bar{\sigma}}d_{\sigma};d^{\dagger}_{\sigma}\rangle\rangle$ (with $\bar{\sigma}=-\sigma$).[28] Upon calculating the averages $\langle a^{\dagger}_{m\sigma}a_{m'\sigma}\rangle$ and $\langle d^{\dagger}_{\sigma}a_{m\sigma}\rangle$ using Eq. (7), the set of EOM is closed, and can be therefore solved. The details of this calculation are presented in Appendix A. In particular, the resulting equation determining the dot Green function is

$$G_{\sigma}(z)=\frac{u(z)-\langle n_{d\bar{\sigma}}\rangle-P_{\bar{\sigma}}(z_1)-P_{\bar{\sigma}}(z_2)}{u(z)[z-\epsilon_0-\sigma h-\Sigma_{\sigma}(z)]+[P_{\bar{\sigma}}(z_1)+P_{\bar{\sigma}}(z_2)]\Sigma_{\sigma}(z)-Q_{\bar{\sigma}}(z_1)+Q_{\bar{\sigma}}(z_2)}, \tag{9}$$

where

$$u(z)\equiv U^{-1}[U-z+\epsilon_0+\sigma h+\Sigma_{\sigma}(z)+\Sigma_{\bar{\sigma}}(z_1)-\Sigma_{\bar{\sigma}}(z_2)], \tag{10}$$

and $z_1\equiv z-2\sigma h$, $z_2\equiv -z+2\epsilon_0+U$. The functions P and Q are given in terms of the noninteracting self-energy on the dot, $\Sigma_{\sigma}(z)$, brought about by its coupling to the network [namely, the self-energy of the noninteracting dot, see Eq. (A7)], and the dot Green function itself [see Eqs. (A25)],

$$P_{\sigma}(z)=\mathfrak{F}_{\sigma z}[G],\quad Q_{\sigma}(z)=\mathfrak{F}_{\sigma z}[1+\Sigma G], \tag{11}$$

where the notation $\mathfrak{F}_{\sigma z}[g]$ stands for

$$\mathfrak{F}_{\sigma z}[g]\equiv\frac{i}{2\pi}\oint_C f(w)g_{\sigma}(w)\frac{\Sigma_{\sigma}(w)-\Sigma_{\sigma}(z)}{z-w}dw. \tag{12}$$

Equation (9) generalizes the result of Ref. 11 (see also Refs. 18–21) for the case in which the interaction on the dot is finite, and the entire system is subject to an external magnetic field. Our generalization also corrects a few details in Lacroix's earlier treatment of finite U.[12]

III. PROPERTIES OF THE EOM APPROXIMATION AT FINITE U

As is evident from Eq. (9), the solution of the dot Green function within the EOM scheme cannot be easily obtained over the entire parameter range. However, there are certain limiting cases in which this Green function can be analyzed analytically. We examine those in the subsequent sections.

A. Particle-hole symmetry

Upon replacing the particle operators by the hole ones, $\tilde{d}^{\dagger}_{\sigma}\equiv d_{\sigma}, \tilde{a}^{\dagger}_{n\sigma}\equiv a_{n\sigma}$, the Anderson Hamiltonian (1) attains its original structure, with

$$\tilde{\epsilon}_0+\sigma\tilde{h}=-\epsilon_0-\sigma h-U,\quad \tilde{U}=U,$$

$$\tilde{J}_{n\sigma}=-J^{*}_{n\sigma},\quad \tilde{\varepsilon}_{n\sigma}=-\varepsilon_{n\sigma},\quad \tilde{J}_{nm}=-J_{mn}. \tag{13}$$

(Hole quantities are denoted by a tilde.) The dot Green function in terms of the hole operators is then related to the particle Green function by

$$\tilde{G}_{\sigma}(z)\equiv\langle\langle\tilde{d}_{\sigma};\tilde{d}^{\dagger}_{\sigma}\rangle\rangle_z=-G_{\sigma}(-z). \tag{14}$$

One may check that this equivalence holds by introducing the definitions (13) into Eq. (9). Since $\tilde{\Sigma}_{\sigma}(z)=-\Sigma_{\sigma}(-z)$ and $\tilde{u}(z)=1-u(-z)$, one finds that [see Eqs. (A25) and (A26)] $\tilde{P}_{\sigma}(z)=-P_{\sigma}(-z)$ and $\tilde{Q}_{\sigma}(z)=Q_{\sigma}(-z)-\Sigma_{\sigma}(-z)$, reconfirming Eq. (14).

From now on we shall assume that $\Sigma_{\sigma}(z)=-\Sigma_{\sigma}(-z)$. This relation is realized, for example, when the network to which the dot is coupled has a wide band spectrum, with the Fermi level at the middle. We next discuss the particular point where $2\epsilon_0+U=0$ and $h=0$. At this point, the Anderson Hamiltonian becomes *particle-hole symmetric*. Then $G_{\sigma}(z)=-G_{\sigma}(-z)$, $P_{\sigma}(z)+P_{\sigma}(-z)=0$, $Q_{\sigma}(z)-Q_{\sigma}(-z)=\Sigma_{\sigma}(z)$, and $\langle n_{d\sigma}\rangle=1/2$. As a result, Eq. (9) becomes

$$[G_{\sigma}(z)]^{-1}=z-\Sigma_{\sigma}(z)-\frac{U^2}{4[z-\Sigma_{\sigma}(z)-2\Sigma_{\bar{\sigma}}(z)]}. \tag{15}$$

Namely, at the particle-hole symmetry point of the Anderson model, the EOM results in a *temperature-independent* dot Green function. This implies that the EOM technique at the particle-hole symmetric point *cannot* produce the Kondo singularity. This property of the EOM scheme has been reported a long time ago,[10,29,30] but was ignored in more modern uses of it,[5] which are designed to study the Kondo peak in the density of states.

The failure of the EOM method to describe faithfully the Anderson model at its symmetric point, where the Fermi level lies *exactly* between the states of single and double occupancies, is a very severe drawback of this method. An important question is whether this point is either a singular or a continuous domain, which the EOM method fails totally. We return to this problem in the next section.

B. Zero-temperature relations

The zero-temperature limit is of special importance since the Green function *at the Fermi energy* at $T=0$ satisfies the Fermi-liquid relations[4,31]

$$\mathrm{Im}\,[G^{+}_{\sigma}(0)]^{-1}=\Gamma_{\sigma}, \tag{16}$$

$$\mathrm{Re}[G_\sigma^+(0)]^{-1} = -\Gamma_\sigma \cot(\pi \tilde{n}_{d\sigma}). \quad (17)$$

Here and below we use $A^\pm(\omega) \equiv \lim_{\eta\to\pm 0} A(\omega + i\eta)$, so that $G_\sigma^+(\omega) = [G_\sigma^-(\omega)]^*$ is the usual retarded Green function. In Eqs. (16) and (17), Γ_σ is the level broadening,

$$\Gamma_\sigma \equiv -\mathrm{Im}\,\Sigma_\sigma^+(0). \quad (18)$$

The first relation, Eq. (16), implies[31] number conservation, and therefore is sometimes referred to as the "unitarity" condition. The second one, Eq. (17), is the Friedel sum-rule, in which $\tilde{n}_{d\sigma}$ is the total number of spin σ electrons introduced by the quantum dot,[31]

$$\tilde{n}_{d\sigma} = -\frac{1}{\pi}\,\mathrm{Im}\int f(\omega)\left[1 - \frac{\partial \Sigma_\sigma^+(\omega)}{\partial \omega}\right] G_\sigma^+(\omega) d\omega. \quad (19)$$

When the self-energy Σ_σ does not depend on the energy, $\tilde{n}_{d\sigma}$ coincides with the single-spin occupation number on the dot, $\langle n_{d\sigma}\rangle$.

It is evident that the EOM solution for the Green function *at the particle-hole symmetric point*, Eq. (15), *violates* the unitarity condition (16). On the Fermi level, the particle-hole symmetric Green function is

$$[G_\sigma^+(0)]^{-1} = i\Gamma_\sigma + i\frac{U^2}{4(\Gamma_\sigma + 2\Gamma_{\bar\sigma})}, \quad (20)$$

and therefore the imaginary part of $[G_\sigma^+(0)]^{-1}$ is *not* determined solely by the noninteracting self-energy (as implied by the unitarity condition), but has also a contribution coming from the interaction. This is contrary to the result of Lacroix,[12] whose EOM differs from our Eq. (9) in several places. On the other hand, the Friedel sum-rule is satisfied by the Green function (15), which yields $\tilde{n}_{d\sigma} = \frac{1}{2}$. This follows from Eq. (19): The imaginary parts of both $G_\sigma(\omega)$ and $\Sigma_\sigma(\omega)$ are even in ω, while (at the symmetric point) the real parts are odd in it. However, $G_\sigma(\omega) \simeq \omega^{-1}$ at large frequencies, whereas $\partial\Sigma_\sigma(\omega)/\partial\omega \simeq \omega^{-2}$. As a result, the second term in the square brackets of Eq. (19) does not contribute. With $\tilde{n}_{d\sigma} = \frac{1}{2}$, the Friedel sum-rule gives $\mathrm{Re}[G_\sigma^+(0)]^{-1} = 0$, which is fulfilled by Eq. (20).

It is rather intricate to study the full EOM solution, Eq. (9), at $T=0$, even on the Fermi level. However, there are cases in which this can be accomplished without constructing the full solution. The investigation of these cases will also allow us to examine the behavior of $G_\sigma(0)$ as the particle-hole symmetric point is approached. To this end we note that at $T=0$ the functions $P(\omega)$ and $Q(\omega)$ acquire logarithmic singularities as $\omega \to 0$,

$$P_\sigma^\pm(\omega) \sim -\frac{1}{\pi}\Gamma_\sigma G_\sigma^\mp(0)\ln|\omega| + \mathcal{O}(1),$$

$$Q_\sigma^\pm(\omega) \sim -\frac{1}{\pi}\Gamma_\sigma[1 + \Sigma_\sigma^\mp(0)G_\sigma^\mp(0)]\ln|\omega| + \mathcal{O}(1). \quad (21)$$

Therefore, we may examine special points at which the functions P and Q are divergent, keeping only the divergent terms in Eq. (9). Then, that equation reduces to an algebraic one, which can be easily solved to yield G_σ at those special points.

Let us first consider the case in which the Zeeman field h on the dot vanishes, but $2\epsilon_0 + U \neq 0$. Using Eqs. (21) in Eq. (9) yields

$$[G_\sigma^+(0)]^{-1} + \Sigma_\sigma^+(0) = [G_{\bar\sigma}^-(0)]^{-1} + \Sigma_{\bar\sigma}^-(0). \quad (22)$$

By writing the Green function in the general form

$$[G_\sigma(z)]^{-1} = z - \epsilon_0 - \sigma h - \Sigma_\sigma(z) - \Sigma_\sigma^{\mathrm{int}}(z), \quad (23)$$

in which Σ^{int} is the self-energy due to the interaction, Eq. (22) takes the form

$$\Sigma_\sigma^{\mathrm{int}+}(0) - \Sigma_{\bar\sigma}^{\mathrm{int}-}(0) = 0. \quad (24)$$

When the network is not spin polarized, the spin indices σ and $\bar\sigma$ are indistinguishable. Then Eq. (22) implies that $\mathrm{Im}\,\Sigma^{\mathrm{int}}(0)$ vanishes, namely the unitarity condition is satisfied. (In the more general case of possibly ferromagnetic leads, it is only the imaginary part of $[G_\sigma^+(0)]^{-1} - [G_{\bar\sigma}^-(0)]^{-1}$ which is determined by the noninteracting self-energy alone.) Had we now sent $2\epsilon_0 + U$ to zero, we would have found that the EOM result at the particle-hole symmetric point *does* satisfy the unitarity condition, in contradiction to our finding, Eq. (20), above. We thus conclude that the failure of the EOM to obey the Fermi-liquid relation (16) at the symmetric point is *confined* to the symmetric point alone, namely, the imaginary part of Σ^{int} on the Fermi level has a discontinuity.

Next we consider the case where $2\epsilon_0 + U = 0$, but $h \neq 0$. Using Eqs. (21) in Eq. (9) we now find the relation

$$[G_\sigma^+(0)]^{-1} + \Sigma_\sigma^+(0) = -\{[G_{\bar\sigma}^+(0)]^{-1} + \Sigma_{\bar\sigma}^+(0)\}. \quad (25)$$

Inserting here expression (23), we rewrite this relation in the form

$$\Sigma_\sigma^{\mathrm{int}+}(0) + \Sigma_{\bar\sigma}^{\mathrm{int}+}(0) = U. \quad (26)$$

Therefore, $\mathrm{Im}\,\Sigma^{\mathrm{int}}(0) = 0$, in agreement with the unitarity condition. Sending now the Zeeman field on the dot to zero, yields the result $2\mathrm{Re}\,\Sigma^{\mathrm{int}}(0) = U$, which agrees with the real part of Eq. (20). Thus the EOM result for the real part of Σ^{int} on the Fermi energy does not have a discontinuity. We hence conclude that the EOM technique's failure at the symmetric point is confined to the imaginary part of the interacting self-energy alone and to the symmetric point alone.

Our considerations in this subsection are confined to $\omega = 0$, and therefore do not allow us to investigate the Friedel sum-rule easily. We carry out such an analysis for the infinite-U case below. Alternatively, one may attempt, as has been done in Ref. 21, to *impose* the Friedel sum-rule on the EOM result, assuming that Eq. (17) holds, with $\tilde{n}_{d\sigma} \equiv \langle n_{d\sigma}\rangle$. This is a dangerous procedure, which leads in some cases to unphysical results, as is demonstrated in Sec. V.

IV. EXACT SOLUTION IN THE $U \to \infty$ LIMIT

In this section we present an exact solution of the self-consistently truncated EOM, and obtain the dot Green function, in the limit $U \to \infty$. For this solution, we assume that the

bandwidth D_σ is larger than the other energies in the problem (except U). In the next section we use this function to calculate several physical quantities, and compare the results with those of the Bethe ansatz technique and other calculations. For simplicity, we also assume that the noninteracting self-energy may be approximated by an energy-independent resonance width, i.e.,

$$\Sigma_\sigma^\pm = \mp i\Gamma_\sigma, \tag{27}$$

for all the energies in the band, $-D_\sigma < \omega < D_\sigma$ (the extension to the case where there is also an energy-independent real part to the self-energy is straightforward). This assumption is certainly reasonable for a range of energies near the center of the band. However, using it for the whole band introduces corrections of order $|\omega/D_\sigma|$, thus restricting the solution to $|\omega/D_\sigma| \ll 1$. Then, Eq. (9) for the Green function, together with the definitions (10)–(12), takes the form

$$[\mathcal{G}_\sigma^\pm(\omega)]^{-1} G_\sigma^\pm(\omega + \sigma h) = 1 - \langle n_{d\bar\sigma}\rangle - P_{\bar\sigma}^\pm(\omega + \bar\sigma h), \tag{28}$$

where

$$\mathcal{G}_\sigma^\pm(\omega) = [\omega - \epsilon_0 \pm i\Gamma_\sigma - I_{\bar\sigma}^\pm(\omega + \bar\sigma h) \mp i(\Gamma_{\bar\sigma} + \Gamma_\sigma) P_{\bar\sigma}^\pm(\omega + \bar\sigma h)]^{-1}. \tag{29}$$

Note the shift of energies by σh, compared to Eq. (9). The function I_σ introduced here contains the Kondo singularity,[32]

$$I_\sigma^\pm(\omega) = \frac{\Gamma_\sigma}{\pi} \int_{-D_\sigma}^{D_\sigma} d\omega' \frac{f(\omega')}{\omega \pm i\eta - \omega'}. \tag{30}$$

To order $\mathcal{O}(\omega/D_\sigma)$, one has

$$\pi I_\sigma^\pm(\omega)/\Gamma_\sigma = -\Psi\left(\frac{1}{2} \mp \frac{i\omega}{2\pi T}\right) + \ln\frac{D_\sigma}{2\pi T} \mp \frac{i\pi}{2}, \tag{31}$$

where Ψ is the digamma function. Equation (28) for the Green function also contains the function P_σ, which, using the assumption (27), is given by

$$P_\sigma^\pm(\omega) = \frac{\Gamma_\sigma}{\pi} \int_{-D_\sigma}^{D_\sigma} d\omega' \frac{f(\omega') G_\sigma^\mp(\omega')}{\omega \pm i\eta - \omega'} d\omega'. \tag{32}$$

Physically, all the integrals which contain Σ_σ must be calculated between $-D_\sigma$ and D_σ, and the resulting Green function is calculated only for energies inside the band, $|\omega| < D_\sigma$. However, the integral $P_\sigma^\pm(\omega)$ converges even when one takes the limit $D_\sigma \to \infty$, because $G_\sigma(\omega) \sim 1/\omega$ at large $|\omega|$ [see, e.g., Eq. (28)]. If D_σ is sufficiently large, so that this asymptotic behavior becomes accurate and since $f(\omega) \approx 1$ for $\omega < -D_\sigma$, it is convenient to extend the range of this integral (and all the related integrals below, unless otherwise specified) to the range $-\infty < \omega < \infty$. This introduces errors of order Γ_σ/D_σ or ω/D_σ in the results, which we neglect.

We have thus found that the equation for G_σ^+ involves an integral containing the function $G_{\bar\sigma}^-$, and thus the two functions G_σ^+ and $G_{\bar\sigma}^-$ are coupled. In addition, the occupations $\langle n_{d\sigma}\rangle$ have to be determined self-consistently from the Green functions themselves. Our solution for the Green function follows the method introduced in Refs. 10 and 33. This method allows one to turn the integral equations into algebraic ones, at the cost of additional quantities which have to be determined self-consistently from the Green function. First, one introduces the functions

$$\Phi_\sigma(z) = z - \epsilon_0 + i\Gamma_\sigma - I_{\bar\sigma}(z + \bar\sigma h) - i(\Gamma_{\bar\sigma} + \Gamma_\sigma)\frac{\Gamma_{\bar\sigma}}{\pi} \times \int d\omega' \frac{f(\omega') G_{\bar\sigma}^-(\omega')}{z + \bar\sigma h - \omega'},$$

$$\tilde\Phi_\sigma(z) = z - \epsilon_0 - i\Gamma_{\bar\sigma} - I_\sigma(z + \sigma h) + i(\Gamma_{\bar\sigma} + \Gamma_\sigma)\frac{\Gamma_\sigma}{\pi} \times \int d\omega' \frac{f(\omega') G_\sigma^+(\omega')}{z + \sigma h - \omega'}. \tag{33}$$

Note that $\Phi_\sigma^+(\omega)$ is identical to $[\mathcal{G}_\sigma^+(\omega)]^{-1}$ and $\tilde\Phi_\sigma^-(\omega) \equiv [\mathcal{G}_{\bar\sigma}^-(\omega)]^{-1}$, while $\Phi_\sigma^-(\omega)$ and $\tilde\Phi_\sigma^+(\omega)$ are *different* from $[\mathcal{G}_\sigma^-(\omega)]^{-1}$ and $[\mathcal{G}_{\bar\sigma}^+(\omega)]^{-1}$, respectively. The knowledge of $\Phi_\sigma^\pm$ is sufficient to determine $G_{\bar\sigma}^-$, since

$$\Phi_\sigma^+(\omega) - \Phi_\sigma^-(\omega) = 2i\Gamma_{\bar\sigma} f(\omega + \bar\sigma h)[1 + i(\Gamma_{\bar\sigma} + \Gamma_\sigma) G_{\bar\sigma}^-(\omega + \bar\sigma h)]. \tag{34}$$

Similarly, the functions $\tilde\Phi_\sigma^\pm$ determine G_σ^+, through the relation

$$\tilde\Phi_\sigma^+(\omega) - \tilde\Phi_\sigma^-(\omega) = 2i\Gamma_\sigma f(\omega + \sigma h)[1 - i(\Gamma_{\bar\sigma} + \Gamma_\sigma) G_\sigma^+(\omega + \sigma h)]. \tag{35}$$

Returning now to Eq. (28), we eliminate the Green functions by using Eqs. (34) and (35), and the functions P by using the definitions (33). In this way we find

$$\Phi_\sigma^+(\omega)\frac{\tilde\Phi_\sigma^+(\omega) - \tilde\Phi_\sigma^-(\omega)}{2i\Gamma_\alpha f(\omega + \sigma h)} = \mathrm{X}_\sigma^+(\omega),$$

$$\tilde\Phi_\sigma^-(\omega)\frac{\Phi_\sigma^+(\omega) - \Phi_\sigma^-(\omega)}{2i\Gamma_{\bar\alpha} f(\omega + \bar\sigma h)} = \tilde{\mathrm{X}}_\sigma^-(\omega), \tag{36}$$

where

$$\mathrm{X}_\sigma(z) = -i(\Gamma_\sigma + \Gamma_{\bar\sigma})(1 - \langle n_{d\bar\sigma}\rangle) + z - \epsilon_0 + i\Gamma_\sigma - I_{\bar\sigma}(z + \bar\sigma h),$$

$$\tilde{\mathrm{X}}_\sigma(z) = i(\Gamma_\sigma + \Gamma_{\bar\sigma})(1 - \langle n_{d\sigma}\rangle) + z - \epsilon_0 - i\Gamma_{\bar\sigma} - I_\sigma(z + \sigma h). \tag{37}$$

So far, we have not achieved much simplification over the original problem at hand. However, noting that

$$\mathrm{X}_\sigma^+(\omega) - \mathrm{X}_\sigma^-(\omega) = 2i\Gamma_{\bar\alpha} f(\omega + \bar\sigma h),$$

$$\tilde X_\sigma^+(\omega) - \tilde X_\sigma^-(\omega) = 2i\Gamma_\alpha f(\omega + \sigma h), \tag{38}$$

Eqs. (36) yield the remarkable result

$$\Phi_\sigma^+(\omega)\tilde{\Phi}_\sigma^+(\omega) - X_\sigma^+(\omega)\tilde{X}_\sigma^+(\omega) = \Phi_\sigma^-(\omega)\tilde{\Phi}_\sigma^-(\omega) - X_\sigma^-(\omega)\tilde{X}_\sigma^-(\omega). \tag{39}$$

Therefore, the combination

$$R(z) \equiv \Phi_\sigma(z)\tilde{\Phi}_\sigma(z) - X_\sigma(z)\tilde{X}_\sigma(z) \tag{40}$$

is *nonsingular* across the real axis. In fact, the only singular point of this combination is at $z=\infty$. This means that $R(z)$ can be written as a polynomial with non-negative powers of z. Moreover, since Φ, $\tilde{\Phi}$, X, and $\tilde{X}$ grow only linearly as $z \to \infty$, that polynomial includes only two terms, $r_0+r_1 z$. The details of this calculation are given in Appendix B. The result (39) allows one to express the (unknown) functions Φ and $\tilde{\Phi}$ in terms of the (known) functions X, $\tilde{X}$, and R,

$$\frac{\Phi_\sigma^+}{\Phi_\sigma^-} = \frac{R + X_\sigma^+\tilde{X}_\sigma^-}{R + X_\sigma^-\tilde{X}_\sigma^-} \equiv H_\sigma(\omega), \quad \frac{\tilde{\Phi}_\sigma^+}{\tilde{\Phi}_\sigma^-} = \frac{R + X_\sigma^+\tilde{X}_\sigma^+}{R + X_\sigma^-\tilde{X}_\sigma^-} \equiv \tilde{H}_\sigma(\omega). \tag{41}$$

This reduces our problem into two independent *linear Reimann-Hilbert problems*, for which a rigorous solution is available,[33,34]

$$\Phi_\sigma(z) = (z-a)e^{M_\sigma(z)}, \quad M_\sigma(z) = \int \left(-\frac{d\omega}{2\pi i}\right)\frac{\ln H_\sigma(\omega)}{z-\omega},$$

$$\tilde{\Phi}_\sigma(z) = (z-\tilde{a})e^{\tilde{M}_\sigma(z)}, \quad \tilde{M}_\sigma(z) = \int \left(-\frac{d\omega}{2\pi i}\right)\frac{\ln \tilde{H}_\sigma(\omega)}{z-\omega}. \tag{42}$$

This is a valid solution as long as $\ln H(\omega)$ and $\ln \tilde{H}(\omega)$ can be chosen to be continuous in ω and to vanish at both ends of the integration interval.[35] All the cases studied in this paper obey this requirement, although we could not prove the absence of solutions other than (42) for a general case with no spin symmetry. The form of the polynomial prefactors, $(z-a)$ and $(z-\tilde{a})$, in Eq. (42) is dictated by the fact that the leading term in $\Phi_\sigma(z)$ and $\tilde{\Phi}_\sigma(z)$ must be z [see Eqs. (33)]. The determination of the coefficients a and $\tilde{a}$, as well as other self-consistent quantities, is detailed in Appendix C.

V. PHYSICAL PROPERTIES IN THE $U \to \infty$ LIMIT

Once the functions Φ and $\tilde{\Phi}$ are found, then the Green function is determined from Eq. (34) or Eq. (35). This knowledge enables us to compute various physical quantities, and compare them with the results of other calculations. The first quantity we consider is the total occupation on the dot, $n_0 \equiv \langle n_{d\uparrow} + n_{d\downarrow}\rangle$, at zero temperature. This calculation is carried out for the spin-symmetric case, $h=0$ and spin-independent self-energy. We also denote $D \equiv D_\sigma$, $\Gamma \equiv \Gamma_\sigma$. The result is plotted as function of E_d/Γ, where

$$E_d \equiv \epsilon_0 + (\Gamma/\pi)\ln(D/\Gamma), \tag{43}$$

and is portrayed in Fig. 1 (full line). It agrees within 3% with the exact universal curve $n_0(E_d/\Gamma)$, as found from the Bethe ansatz,[36] (open circles). Thus, the EOM solution conforms with Haldane's scaling.[37] On the other hand, the EOM solution fails to satisfy the Friedel sum-rule, as has been already discussed above.[38] The total occupation calculated from Eq. (17) (dashed line) deviates systematically from the self-consistent values, in particular in the Kondo regime $(n_0 \to 1)$. Note that Eq. (27) implies that $\tilde{n}_{d\sigma} = \langle n_{d\sigma}\rangle$ [see Eq. (19)].

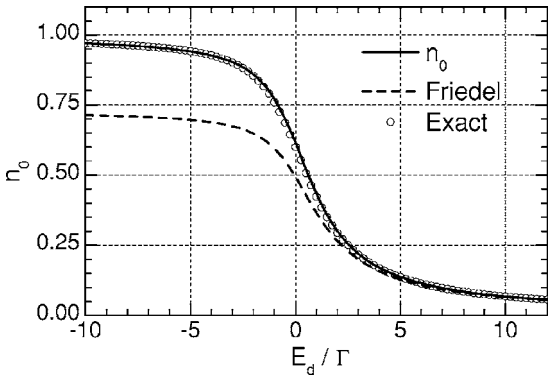

FIG. 1. The zero-temperature occupation number n_0 as function of the renormalized energy E_d calculated self-consistently by the EOM method (solid line), and from the Friedel sum-rule, Eq. (17) (dashed line). Open circles show the exact Bethe ansatz results (Ref. 36).

As mentioned above, the Fermi-liquid relations are connected with unitarity. In particular, at zero temperature the linear conductance of a symmetrically coupled quantum dot is given by[3,5] $-2(e^2/h)\Gamma_\sigma \operatorname{Im} G_\sigma(\omega=0)$. Thus, the unitary limit $2e^2/h$ is reached only if $\operatorname{Re}[G_\sigma^+(0)] \to 0$ and the Fermi liquid relation (16) holds. As implied by the dashed line in the figure, the first of these criteria is not obeyed by the self-consistent solution.

Next we consider the local spin susceptibility on the dot. When the leads are nonmagnetic, this quantity is given by $\chi = \frac{1}{2}(g\mu_B)^2 \partial\langle n_{d\downarrow} - n_{d\uparrow}\rangle/\partial h$, with $h = -g\mu_B B$. Here B is the external magnetic field and $g\mu_B$ is the gyromagnetic ratio of electrons in the quantum dot. [The spin susceptibility of the leads adds to the local susceptibility the usual Pauli term, and $\mathcal{O}(\Gamma_\sigma/D_\sigma)$ corrections.[4]] We have calculated $\chi(E_d/\Gamma, T)$ by differentiating the self-consistent equations for $\langle n_{d\sigma}\rangle$ with respect to h, and evaluating the integrals numerically. This procedure is similar to the one which has been used for the Wolff model in Ref. 10(b), but is free from numerical accuracy problems reported there.

The zero-temperature susceptibility derived from the EOM is found to be in a good *quantitative* agreement with the Bethe ansatz results in the mixed valence $(|E_d/\Gamma| \lesssim 1)$ and empty orbital $(E_d \gg \Gamma)$ regimes, as is shown in Fig. 2. In the local moment regime, $E_d \ll -\Gamma$, a screening cloud is expected to form due to the Kondo effect at[4,37] $T < T_K \sim \Gamma e^{\pi E_d/(2\Gamma)}$, leading to a crossover from a high-temperature Curie law, $\chi \sim (g\mu_B)^2/T$, to a finite ground state value, $\chi \sim (g\mu_B)^2/T_K$. The latter is underestimated by our self-consistent solution, as is manifested by the deviation from the exact Bethe ansatz results depicted in Fig. 2.

Indeed, had we defined the Kondo temperature through the inverse of the zero-temperature susceptibility, we would

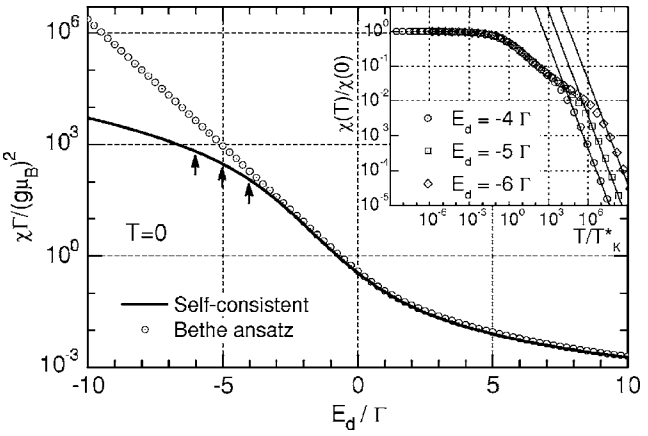

FIG. 2. The local spin susceptibility χ as function of the renormalized energy level E_d, for $T=0$. The EOM result (solid line) is close to the Bethe ansatz one (Ref. 36) (circles) in the empty orbital and mixed valence regimes, but deviates significantly in the strongly correlated region (large negative values of E_d/Γ). Inset: The scaling of the susceptibility with T/T_K^* at three fixed energy level positions (marked by arrows in the main graph). The solid lines indicate the high-temperature asymptotic behavior, $\chi(T)=(g\mu_B)^2/(6T)$.

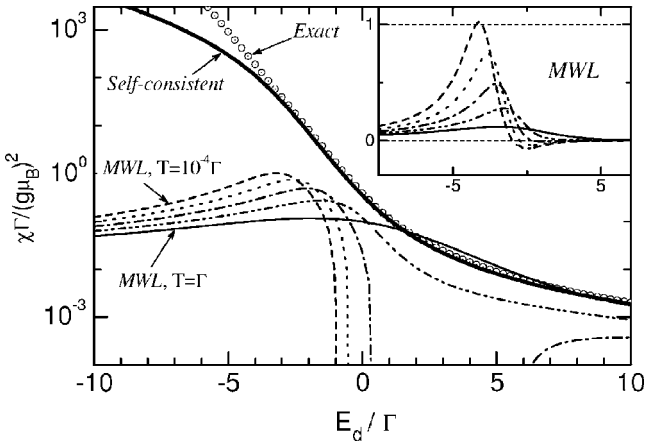

FIG. 3. Data from Fig. 2 compared to the spin susceptibility given by the MWL approximation in the temperature range from $T=1\Gamma$ down to $T=10^{-4}\Gamma$. The inset shows the MWL susceptibilities only, on a linear scale, allowing for the negative values.

have found that the EOM method *overestimates* that temperature. However, within EOM, the relevant energy scale is determined from the leading (real) terms in the denominator of the Green function, i.e., by the temperature at which the real part of $\mathcal{G}$, Eq. (29), vanishes. Using for $I(z)$, Eq. (31), the approximate form[9] $I(z)\approx-(\Gamma/\pi)\ln[(z+i\kappa T)/D]$ where κ is a number of order unity, we find that the leading terms are

$$\omega - E_d + \frac{\Gamma}{\pi}\ln\frac{D}{\Gamma} + \frac{\Gamma}{\pi}\ln\frac{\sqrt{\omega^2+\kappa^2T^2}}{D}, \tag{44}$$

yielding for the temperature scale

$$T_K^* \sim \Gamma e^{\pi E_d/\Gamma}, \tag{45}$$

such that the leading terms are

$$\omega + \frac{\Gamma}{\pi}\ln\sqrt{(\omega/T_K^*)^2+(\kappa T/T_K^*)^2}. \tag{46}$$

The logarithm in Eq. (46) dominates the properties of the solution close to the Fermi energy at temperatures $T\lesssim T_K^*$. The same energy scale T_K^* has been determined from the analysis of the truncated EOM in Refs. 11 and 18. Note that T_K^* is *smaller* than the true Kondo temperature T_K.

The local spin susceptibility at finite temperatures, calculated from our EOM solution, is shown in the inset of Fig. 2. Indeed, $\chi(T)/\chi(0)$ scales with T/T_K^*, but instead of crossing over to the Curie law, a region of intermediate behavior in which $\chi\sim T^x$ with $-1<x<0$ is observed. The high-temperature asymptotic $\chi(T)\sim 1/T$ is approached only for $T\gtrsim\Gamma$. Such a behavior in the intermediate temperature range $T_K^*<T<\Gamma$ is not supported by NRG or Bethe ansatz calculations,[4] which scale with T_K,[39] and has thus to be attributed to the deficiency of the EOM method.

In contrast, neither the Lacroix approximation, as implemented in Ref. 18, nor the MWL[5] approximate Green function leads to comparable results when used to calculate the local spin susceptibility. The Lacroix approximation becomes intrinsically inconsistent at finite magnetic fields, since it results in a logarithmic divergence of $G_\sigma(z)$ as $z\to\sigma h$. Even when ignoring this inconsistency, the zero-temperature spin susceptibility calculated in that approximation attains negative and divergent values regardless of the quantum dot parameters. The MWL approximation leads to finite, but quite unphysical values of χ for $T<\Gamma$, as we demonstrate in Fig. 3. That approximation gives reasonable results at $T=\Gamma$: the susceptibility follows roughly the Curie law $\approx 1/T(=1/\Gamma)$ or the zero-temperature value, whichever is smaller. At lower temperatures one would have expected a gradual increase in the susceptibility in the Kondo region. Instead, a window of a *negative susceptibility* opens, which is widened as the temperature is decreased. At strictly zero temperature χ is negative for all values of E_d. This example shows the necessity of using the full self-consistency of the EOM solution in order to obtain the qualitatively correct behavior.

Finally, we examine the local density of states on the dot, given by

$$\rho(\omega,T) \equiv -\,\mathrm{Im}\sum_\sigma G_\sigma^+(\omega)/\pi, \tag{47}$$

as calculated from the EOM. The inset of Fig. 4 shows the Kondo peak at temperatures $T\lesssim T_K^*$. The local density of states at the Fermi energy follows the universal temperature dependence, as can be seen in Fig. 4, with the same scaling factor T_K^* as the spin susceptibility (compare to the inset of Fig. 2). The appearance of a single scale determining the low-energy properties of the system is another hallmark[4] of the Kondo effect which is captured by the fully self-consistent EOM technique.

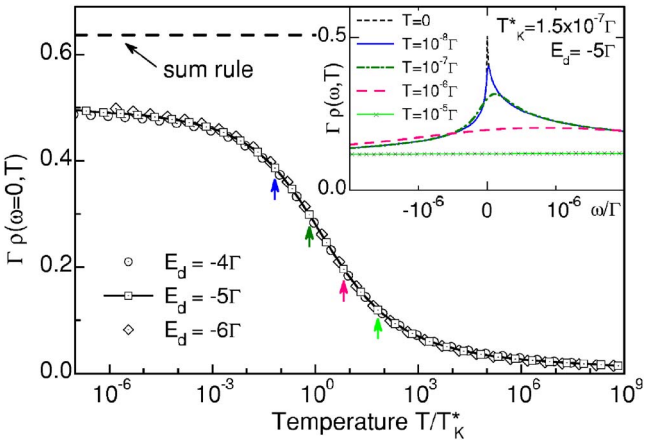

FIG. 4. (Color online) The scaling of the local density of states at the Fermi level as function of the reduced temperature T/T_K^*, is demonstrated by plotting $\rho(\omega=0,T)$ for three different values of the renormalized single-electron energy on the dot, E_d [Eq. (43)]. The dashed line at $\rho=2/(\pi\Gamma)$ corresponds to the limit dictated by the Friedel sum-rule at $E_d/\Gamma \ll -1$. The inset shows the melting of the Kondo peak as the temperature is increased at fixed $E_d/\Gamma=-5$. Temperature values represented in the inset are marked by arrows in the main graph.

VI. PERTURBATION EXPANSION IN THE DOT-NETWORK COUPLINGS

The EOM technique is unfortunately not a systematic expansion. It is therefore very interesting to compare its results with those given by a direct expansion. Here we expand the EOM Green function up to second order in the dot-network couplings $J_{n\sigma}$. For compactness, we confine ourselves to the case $U\to\infty$, and assume for simplicity that the noninteracting self-energy has just an energy-independent imaginary part, i.e., $\Sigma_\sigma(\omega)=-i\Gamma_\sigma$. By comparing with the direct perturbation theory expansion[24,25] we find that, up to second order in $J_{n\sigma}$, our EOM result for the dot Green function is exact. (See also Ref. 23.) On the other hand, the Green function derived in Ref. 5 (which does not include all correlations resulting from the truncated EOM) violates the second-order perturbation theory result, and in fact, predicts a Kondo anomaly in this order (which should not be there).

The $U\to\infty$ Green function of the EOM is given by Eqs. (28)–(30) and (32). Since the noninteracting self-energy Σ_σ, and consequently the width Γ_σ are second order in the coupling $J_{n\sigma}$, the expansion of the Green function reads

$$G_\sigma^{(0)}(z)=\frac{\delta n_{\bar\sigma}^{(0)}}{z-\epsilon_\sigma}, \tag{48}$$

and

$$G_\sigma^{(2)}(z)=\frac{\delta n_{\bar\sigma}^{(2)}-P_{\bar\sigma}^{(2)}(z_1)}{z-\epsilon_\sigma}+G_\sigma^{(0)}(z)\frac{I_{\bar\sigma}(z_1)+\Sigma_\sigma(z)}{z-\epsilon_\sigma}, \tag{49}$$

where we have denoted

$$\langle n_{\bar\sigma}\rangle \equiv 1-\delta n_{\bar\sigma}, \quad \epsilon_\sigma=\epsilon_0+\sigma h \tag{50}$$

and where the superscript (k) denotes the contribution of order k in the couplings. The function $P^{(2)}$ is found by using the zeroth-order of the Green function in Eq. (32),

$$P_\sigma^{(2)}(z)=G_\sigma^{(0)}(z)[I_\sigma(z)-I_\sigma^-(\epsilon_\sigma)-f(\epsilon_\sigma)\Sigma_\sigma(z)+f(\epsilon_\sigma)\Sigma_\sigma^-(\epsilon_\sigma)]. \tag{51}$$

Using the identities

$$I_\sigma^-(\epsilon_\sigma)-f(\epsilon_\sigma)\Sigma_\sigma^-(\epsilon_\sigma)=\mathrm{Re}[I_\sigma(\epsilon_\sigma)-f(\epsilon_\sigma)\Sigma_\sigma(\epsilon_\sigma)] \tag{52}$$

and

$$G_{\bar\sigma}^{(0)}(z_1)=\delta n_\sigma^{(0)}G_\sigma^{(0)}(z)/\delta n_{\bar\sigma}^{(0)}, \tag{53}$$

Eq. (49) takes the form

$$G_\sigma^{(2)}(z)=\frac{\delta n_{\bar\sigma}^{(2)}}{z-\epsilon_\sigma}+\frac{-\delta n_\sigma^{(0)}[I_{\bar\sigma}(z_1)-f(\epsilon_{\bar\sigma})\Sigma_{\bar\sigma}(z_1)-\mathrm{Re}\{I_{\bar\sigma}(\epsilon_{\bar\sigma})-f(\epsilon_{\bar\sigma})\Sigma_{\bar\sigma}(\epsilon_{\bar\sigma})\}]+\delta n_{\bar\sigma}^{(0)}[I_{\bar\sigma}(z_1)+\Sigma_\sigma(z)]}{(z-\epsilon_\sigma)^2}. \tag{54}$$

In order to complete the second-order calculation, we need to find the occupation numbers $\delta n_\sigma^{(0)}$ and $\delta n_\sigma^{(2)}$ [see Eq. (50)]. From Eq. (48) we find

$$\langle n_\sigma\rangle^{(0)}=\frac{f(\epsilon_\sigma)[1-f(\epsilon_{\bar\sigma})]}{1-f(\epsilon_\sigma)f(\epsilon_{\bar\sigma})}. \tag{55}$$

The second-order correction to the occupation number, $\delta n_\sigma^{(2)}\equiv-\langle n_\sigma\rangle^{(2)}$, is obtained by integrating over the Fermi function multiplied by the second-order correction to the density of states, $\rho_\sigma^{(2)}(\omega)$. The latter reads

$$\rho_\sigma^{(2)}(\omega)\equiv\frac{G_\sigma^{+(2)}(\omega)-G_\sigma^{-(2)}(\omega)}{-2\pi i}=\delta(\omega-\epsilon_\sigma)\left(\delta n_{\bar\sigma}^{(2)}+[\langle n_\sigma\rangle^{(0)}-\langle n_{\bar\sigma}\rangle^{(0)}]\frac{\partial\,\mathrm{Re}\,I_{\bar\sigma}(\epsilon_{\bar\sigma})}{\partial\epsilon_0}\right)-\delta'(\omega-\epsilon_\sigma)\delta n_{\bar\sigma}^{(0)}\,\mathrm{Re}\,I_{\bar\sigma}(\epsilon_{\bar\sigma})$$
$$+\frac{\Gamma_\sigma+(\Gamma_{\bar\sigma}-\Gamma_\sigma)\langle n_{\bar\sigma}\rangle^{(0)}+\Gamma_{\bar\sigma}f(\omega-\epsilon_\sigma+\epsilon_{\bar\sigma})[\langle n_\sigma\rangle^{(0)}-\langle n_{\bar\sigma}\rangle^{(0)}]}{\pi(\omega-\epsilon_\sigma)^2}. \tag{56}$$

Apart from the terms representing the second-order modifications of the singularity at ϵ_σ [the first and second members of Eq. (56)], our result reproduces the one of Ref. 24, for the case where the width Γ_σ is spin independent, i.e., $\Gamma_\sigma=\Gamma_{\bar{\sigma}}$. Note that this density of states remains finite at all temperatures. The Kondo divergence of $\rho_\sigma^{(k)}(0)$ in the limit $T\to 0$ appears only at $k\geqslant 4$ (see Ref. 24). Using the second-order correction to the density of states, we find

$$\langle n_\sigma\rangle^{(2)} = \int f(\omega)\rho_\sigma^{(2)}(\omega)d\omega = (\langle n_{\bar{\sigma}}\rangle^{(0)} - 1)\mathrm{Re}\,\frac{\partial I_\sigma(\epsilon_\sigma)}{\partial\epsilon_\sigma} + \frac{\partial\langle n_\sigma\rangle^{(0)}}{\partial\epsilon_\sigma}\,\mathrm{Re}\,I_{\bar{\sigma}}(\epsilon_{\bar{\sigma}}) + \frac{\partial\langle n_\sigma\rangle^{(0)}}{\partial\epsilon_{\bar{\sigma}}}\,\mathrm{Re}\,I_\sigma(\epsilon_\sigma). \tag{57}$$

This result is identical to the $U\to\infty$ limit of Eq. (5) in Ref. 25 which was obtained by a direct perturbation expansion. Figure 5 depicts the total occupation, $n_0=\Sigma_\sigma\langle n_\sigma\rangle$, as function of ϵ_0, as found from the EOM technique, and as computed from Eqs. (55) and (57) to first order in the width. The two curves differ by a few percents. The comparison with the exact result is carried out in Sec. IV.

VII. CONCLUSIONS

We have presented a solution for the Green function of an interacting quantum dot embedded in a general noninteracting network. Our solution is derived within the EOM technique, taking into account exactly *all* resulting correlations once those equations are truncated. We have tested our solution by analyzing several limiting cases, and by comparing several physical properties derived from that solution with other results available by the Bethe ansatz method and by NRG computations.

We have found that the EOM Green function is temperature independent at the particle-hole symmetric point (where $h=0$ and $2\epsilon_0+U=0$). We have found that this deficiency of the EOM is related to a discontinuity in the imaginary part of the interacting self-energy at that particular point. However, this imaginary part obeys the Fermi-liquid unitarity requirement away from this special point, at zero temperature. In contrast, even away from the particle-hole symmetric point, the EOM result fails to satisfy the Friedel sum-rule deep inside the Kondo regime, as we have shown explicitly in the infinite interaction limit.

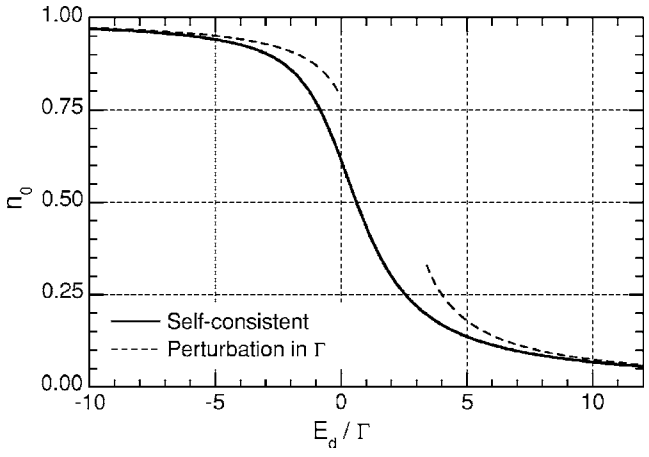

FIG. 5. The equilibrium occupation number $n_0=\Sigma_\sigma\langle n_\sigma\rangle$ for the same parameters as in Fig. 1, and $D=100\Gamma$ (since second-order perturbation theory *does not* scale with E_d, the bandwidth has to be specified), calculated from the self-consistently truncated EOM (solid lines), and by perturbation theory to first order in Γ, Eqs. (55) and (57) (dashed line). The perturbational result diverges at $\epsilon_0=0$.

Albeit these problems, the EOM solution reproduces faithfully the low-temperature scaling of the spin susceptibility and the density of states at the Fermi level, though with an energy scale T_K^* which differs from the true Kondo temperature [cf. Eq. (45)]. Zero-temperature results are in excellent agreement with the exact Bethe ansatz solution, except for the Kondo correlated regime. As the temperature is raised, the EOM results become more and more quantitatively correct, and approach high-temperature asymptotics known rigorously from perturbation theory and NRG studies. We have expanded the EOM Green function to second order in the dot-network coupling and found an exact agreement with direct calculations by perturbation theory. Most importantly, we have found that it is crucial to include in the EOM solution *all* the correlations emerging from the truncated scheme. Ignoring part of these correlations, as is ubiquitously done in such studies, results in erroneous behaviors of various physical quantities.

Hence we conclude that the method examined in this paper can provide a reasonable description of a quantum dot system over a wide parameter range, provided that the self-consistency conditions inherent to this technique are fully taken into account.

ACKNOWLEDGMENTS

We thank A. Schiller for helpful comments. This project was carried out in a center of excellence supported by the Israel Science Foundation.

APPENDIX A: EOM FOR THE FINITE U CASE

Here we extend the derivations of Refs. 9, 13, and 18, carried out for an infinite repulsive interaction, to the case in which U is finite. In addition, we allow for a Zeeman field, assuming that the quantization axes of the spins are the same on the dot and on the leads (but the g factors may be differ-

ent). The Hamiltonian of the our system is given in Eq. (1).

The Fourier transform of the EOM for the Green function defined in Eq. (5) can be written in two alternative forms[8] (both will be used in the following),

$$z\langle\langle A;B\rangle\rangle_z = \langle[A,B]_+\rangle + \langle\langle[A,\mathcal{H}]_-;B\rangle\rangle_z = \langle[A,B]_+\rangle - \langle\langle A;[B,\mathcal{H}]_-\rangle\rangle_z. \tag{A1}$$

It follows that the EOM for the dot Green function is

$$[z-\epsilon_0-\sigma h]G_\sigma = 1 + U\langle\langle n_{d\bar\sigma}d_\sigma;d_\sigma^\dagger\rangle\rangle - \sum_n J_{n\sigma}\langle\langle a_{n\sigma};d_\sigma^\dagger\rangle\rangle, \tag{A2}$$

where $\bar\sigma$ is the spin direction opposite to σ. Here and in the following we frequently omit for brevity explicit indications of the argument z. We first consider the last term on the right-hand side of Eq. (A2). The EOM for the Green function appearing there is

$$(z-\varepsilon_{n\sigma})\langle\langle a_{n\sigma};d_\sigma^\dagger\rangle\rangle = -\sum_m J_{nm}\langle\langle a_{m\sigma};d_\sigma^\dagger\rangle\rangle - J_{n\sigma}^* G_\sigma. \tag{A3}$$

Introducing the inverse matrix

$$\mathcal{M}_{nm\sigma}(z) \equiv [(z-\mathcal{H}_{\rm net}^\sigma)^{-1}]_{nm}, \tag{A4}$$

where $\mathcal{H}_{\rm net}^\sigma$ is the part of $\mathcal{H}_{\rm net}$ pertaining to the spin direction σ, we find

$$\langle\langle a_{n\sigma};d_\sigma^\dagger\rangle\rangle = -\sum_m \mathcal{M}_{nm\sigma}(z)J_{m\sigma}^* G_\sigma. \tag{A5}$$

Note that $\mathcal{M}$ is the Green function matrix of the network *in the absence of the coupling to the dot*. Using Eq. (A5), we find that the last term on the right-hand side of Eq. (A2) can be put in the form

$$-\sum_n J_{n\sigma}\langle\langle a_{n\sigma};d_\sigma^\dagger\rangle\rangle = \Sigma_\sigma G_\sigma, \tag{A6}$$

where

$$\Sigma_\sigma(z) \equiv \sum_{nm} J_{n\sigma}\mathcal{M}_{nm\sigma}(z)J_{m\sigma}^* \tag{A7}$$

is the self-energy of the dot Green function coming from the coupling to the (noninteracting) network. Namely, it is the dot self-energy for the $U=0$ case.[18] As such, it can always be calculated, at least in principle (see, for example, Refs. 18 and 40).

We now turn to the interacting part of the EOM for the dot Green function [the second term on the right-hand side of Eq. (A2)]. The EOM for the four-operator Green function appearing there reads

$$[z-\epsilon_0-\sigma h-U]\langle\langle n_{d\bar\sigma}d_\sigma;d_\sigma^\dagger\rangle\rangle = \langle n_{d\bar\sigma}\rangle - \sum_n [J_{n\sigma}\langle\langle a_{n\sigma}n_{d\bar\sigma};d_\sigma^\dagger\rangle\rangle + J_{n\bar\sigma}\langle\langle d_{\bar\sigma}^\dagger a_{n\bar\sigma}d_\sigma;d_\sigma^\dagger\rangle\rangle - J_{n\bar\sigma}^*\langle\langle a_{n\bar\sigma}^\dagger d_{\bar\sigma}d_\sigma;d_\sigma^\dagger\rangle\rangle], \tag{A8}$$

and gives rise to three new four-operator Green functions (on the right-hand side here). Their EOM are

$$[z-\varepsilon_{n\sigma}]\langle\langle a_{n\sigma}n_{d\bar\sigma};d_\sigma^\dagger\rangle\rangle = -\sum_m J_{nm}\langle\langle a_{m\sigma}n_{d\bar\sigma};d_\sigma^\dagger\rangle\rangle - J_{n\sigma}^*\langle\langle n_{d\bar\sigma}d_\sigma;d_\sigma^\dagger\rangle\rangle - \sum_m [J_{m\bar\sigma}\langle\langle a_{n\sigma}d_{\bar\sigma}^\dagger a_{m\bar\sigma};d_\sigma^\dagger\rangle\rangle - J_{m\bar\sigma}^*\langle\langle a_{m\bar\sigma}^\dagger d_{\bar\sigma}a_{n\sigma};d_\sigma^\dagger\rangle\rangle], \tag{A9}$$

$$[z_1-\varepsilon_{n\bar\sigma}]\langle\langle d_{\bar\sigma}^\dagger a_{n\bar\sigma}d_\sigma;d_\sigma^\dagger\rangle\rangle = \langle d_{\bar\sigma}^\dagger a_{n\bar\sigma}\rangle - \sum_m J_{nm}\langle\langle d_{\bar\sigma}^\dagger a_{m\bar\sigma}d_\sigma;d_\sigma^\dagger\rangle\rangle - J_{n\bar\sigma}^*\langle\langle n_{d\bar\sigma}d_\sigma;d_\sigma^\dagger\rangle\rangle + \sum_m [J_{m\bar\sigma}^*\langle\langle a_{m\bar\sigma}^\dagger a_{n\bar\sigma}d_\sigma;d_\sigma^\dagger\rangle\rangle - J_{m\sigma}\langle\langle d_{\bar\sigma}^\dagger a_{n\bar\sigma}a_{m\sigma};d_\sigma^\dagger\rangle\rangle], \tag{A10}$$

$$[-z_2+\varepsilon_{n\bar\sigma}]\langle\langle a_{n\bar\sigma}^\dagger d_{\bar\sigma}d_\sigma;d_\sigma^\dagger\rangle\rangle = \langle a_{n\bar\sigma}^\dagger d_{\bar\sigma}\rangle + \sum_m J_{nm}^*\langle\langle a_{m\bar\sigma}^\dagger d_{\bar\sigma}d_\sigma;d_\sigma^\dagger\rangle\rangle + J_{n\bar\sigma}\langle\langle n_{d\bar\sigma}d_\sigma;d_\sigma^\dagger\rangle\rangle - \sum_m [J_{m\sigma}\langle\langle a_{n\bar\sigma}^\dagger d_{\bar\sigma}a_{m\sigma};d_\sigma^\dagger\rangle\rangle - J_{m\bar\sigma}\langle\langle a_{n\bar\sigma}^\dagger d_\sigma a_{m\bar\sigma};d_\sigma^\dagger\rangle\rangle], \tag{A11}$$

where we have introduced the definitions

$$z_1 \equiv z-2\sigma h, \quad z_2 \equiv -z+2\epsilon_0+U. \tag{A12}$$

The EOM (A9)–(A11) include four-operator Green functions in which only two of the operators are dot operators. Those are decoupled as detailed in Eq. (8). One then finds

$$-\sum_n J_{n\sigma}\langle\langle a_{n\sigma}n_{\bar\sigma};d_\sigma^\dagger\rangle\rangle = \Sigma_\sigma\langle\langle n_{\bar\sigma}d_\sigma;d_\sigma^\dagger\rangle\rangle + \sum_{nmm'} J_{n\sigma}\mathcal{M}_{nm\sigma}\langle\langle a_{m\sigma};d_\sigma^\dagger\rangle\rangle[J_{m'\bar\sigma}\langle d_{\bar\sigma}^\dagger a_{m'\bar\sigma}\rangle - J_{m'\bar\sigma}^*\langle a_{m'\bar\sigma}^\dagger d_{\bar\sigma}\rangle], \tag{A13}$$

$$-\sum_n J_{n\bar\sigma}\langle\langle d_{\bar\sigma}^\dagger a_{n\bar\sigma}d_\sigma;d_\sigma^\dagger\rangle\rangle = (1+\Sigma_\sigma G_\sigma)P_{\bar\sigma}(z_1) + \Sigma_{\bar\sigma}(z_1)\langle\langle n_{\bar\sigma}d_\sigma;d_\sigma^\dagger\rangle\rangle - G_\sigma Q_{\bar\sigma}(z_1), \tag{A14}$$

$$\sum_n J^*_{n\bar{\sigma}}\langle\langle a^\dagger_{n\bar{\sigma}}d_{\bar{\sigma}}d_\sigma;d^\dagger_\sigma\rangle\rangle = (1+\Sigma_\sigma G_\sigma)P_{\bar{\sigma}}(z_2) - \Sigma_{\bar{\sigma}}(z_2)\langle\langle n_{\bar{\sigma}}d_\sigma;d^\dagger_\sigma\rangle\rangle + G_\sigma Q_{\bar{\sigma}}(z_2), \tag{A15}$$

where we have introduced

$$P_\sigma(z) \equiv -\sum_{nm} J_{n\sigma}\mathcal{M}_{nm\sigma}(z)\langle d^\dagger_\sigma a_{m\sigma}\rangle = -\sum_{mn}\langle a^\dagger_{m\sigma}d_\sigma\rangle\mathcal{M}_{mn\sigma}(z)J^*_{n\sigma}, \tag{A16}$$

$$Q_\sigma(z) \equiv \sum_{nmm'} J_{n\sigma}\mathcal{M}_{nm\sigma}(z)\langle a^\dagger_{m'\sigma}a_{m\sigma}\rangle J^*_{m'\sigma} = \sum_{nmm'} J_{m'\sigma}\langle a^\dagger_{m\sigma}a_{m'\sigma}\rangle\mathcal{M}_{mn\sigma}(z)J^*_{n\sigma}. \tag{A17}$$

The second equality in each of Eqs. (A16) and (A17) is justified below.

Examining Eqs. (A13), (A16), and (A17) reveals that one needs to find thermal averages of two types, the ones belonging to two network operators, $\langle a^\dagger_{m\sigma}a_{m'\sigma}\rangle$, and the ones consisting of a dot and a network operator, $\langle d^\dagger_\sigma a_{m\sigma}\rangle$. These are found [see Eq. (7)] from the corresponding Green's functions, whose EOM are given by Eq. (A3) and

$$(z-\varepsilon_{n\sigma})\langle\langle d_\sigma;a^\dagger_{n\sigma}\rangle\rangle = -\sum_m\langle\langle d_\sigma;a^\dagger_{m\sigma}\rangle\rangle J_{mn} - J_{n\sigma}G_\sigma, \tag{A18}$$

$$(z-\varepsilon_{m\sigma})\langle\langle a_{m\sigma};a^\dagger_{n\sigma}\rangle\rangle = \delta_{mn} - \sum_{m'} J_{mm'}\langle\langle a_{m'\sigma};a^\dagger_{n\sigma}\rangle\rangle - J^*_{m\sigma}\langle\langle d_\sigma;a^\dagger_{n\sigma}\rangle\rangle. \tag{A19}$$

Their solutions in terms of the inverse matrix $\mathcal{M}_{nm\sigma}$ [see Eq. (A4)] are

$$\langle\langle d_\sigma;a^\dagger_{n\sigma}\rangle\rangle = -\sum_m J_{m\sigma}\mathcal{M}_{mn\sigma}G_\sigma, \tag{A20}$$

$$\langle\langle a_{m\sigma};a^\dagger_{n\sigma}\rangle\rangle = \mathcal{M}_{mn\sigma} + \sum_{ln'}\mathcal{M}_{ml\sigma}J^*_{l\sigma}J_{n'\sigma}\mathcal{M}_{n'n\sigma}G_\sigma. \tag{A21}$$

Employing these solutions to obtain the thermal averages appearing in Eq. (A13), we find

$$\sum_{m'} J_{m'\bar{\sigma}}\langle d^\dagger_{\bar{\sigma}}a_{m'\bar{\sigma}}\rangle = \sum_{m'} J^*_{m'\bar{\sigma}}\langle a^\dagger_{m'\bar{\sigma}}d_{\bar{\sigma}}\rangle.$$

Consequently, the terms in the square brackets of Eq. (A13) are cancelled. Next, we use the first equality in each of the definitions (A16) and (A17) together with the auxiliary Green functions (A5) and (A21), to find P and Q in terms of the dot Green function G,

$$P_\sigma(z) = i\oint_C \frac{dz'}{2\pi}f(z')G_\sigma(z') \times\sum_{nm} J_{n\sigma}J^*_{m\sigma}[(z-\mathcal{H}^\sigma_{\rm net})^{-1}(z'-\mathcal{H}^\sigma_{\rm net})^{-1}]_{nm}, \tag{A22}$$

$$Q_\sigma(z) = i\oint_C \frac{dz'}{2\pi}f(z')[1+\Sigma_\sigma(z')G_\sigma(z')] \times\sum_{nm} J_{n\sigma}J^*_{m\sigma}[(z-\mathcal{H}^\sigma_{\rm net})^{-1}(z'-\mathcal{H}^\sigma_{\rm net})^{-1}]_{nm}, \tag{A23}$$

where we have used Eq. (A4). Since

$$(z-\mathcal{H}^\sigma_{\rm net})^{-1}(z-\mathcal{H}^\sigma_{\rm net})^{-1} = \frac{(z'-\mathcal{H}^\sigma_{\rm net})^{-1} - (z-\mathcal{H}^\sigma_{\rm net})^{-1}}{z-z'}, \tag{A24}$$

we can use Eq. (A7) for the noninteracting self-energy, to write the functions P and Q in terms of that self-energy,

$$P_\sigma(z) = \lim_{\eta'\to 0}\frac{i}{2\pi}\int d\omega\frac{f(\omega)}{z-\omega}(G_\sigma(\omega+i\eta')[\Sigma_\sigma(\omega+i\eta')-\Sigma_\sigma(z)] - G_\sigma(\omega-i\eta')[\Sigma_\sigma(\omega-i\eta')-\Sigma_\sigma(z)]) \equiv \frac{i}{2\pi}\oint_C f(w)G_\sigma(w)\frac{\Sigma_\sigma(w)-\Sigma_\sigma(z)}{z-w}dw,$$

$$Q_\sigma(z) = \lim_{\eta'\to 0}\frac{i}{2\pi}\int d\omega\frac{f(\omega)}{z-\omega}([1+\Sigma_\sigma(\omega+i\eta')G_\sigma(\omega+i\eta')][\Sigma_\sigma(\omega+i\eta')-\Sigma_\sigma(z)] - [1+\Sigma_\sigma(\omega-i\eta')G_\sigma(\omega-i\eta')] \times[\Sigma_\sigma(\omega-i\eta')-\Sigma_\sigma(z)]) \equiv \frac{i}{2\pi}\oint_C f(w)[1+\Sigma_\sigma(w)G_\sigma(w)]\frac{\Sigma_\sigma(w)-\Sigma_\sigma(z)}{z-w}dw. \tag{A25}$$

Here and elsewhere the imaginary part of z is always greater than η', so that the contour C never encircles the pole at $w=z$. Note that using the same procedure employing the second equalities in Eqs. (A16) and (A17) gives again Eqs. (A22) and (A23), thus proving that the two definitions of P and Q in Eqs. (A16) and (A17) are equivalent. Equation (A8) can be now easily solved. Inserting the solution into Eq. (A2) leads to the expression for the dot Green function, Eq. (9).

In treating the functions P and Q in Sec. III A we have employed several properties of the complex integrals appearing in Eqs. (A25). Consider, for example, the integral

$$\frac{i}{2\pi}\oint_C G(w)\frac{\Sigma(w)-\Sigma(z)}{z-w}dw. \tag{A26}$$

Since $G(w)$ and $\Sigma(w)$ have no singularities except for a cut along the real axis, it is expedient to complete each half of the contour C by a large-radius semicircle in the upper and lower half-planes. Then, by the residue theorem, Eq. (A26) vanishes provided that $G(w)$ falls as w^{-1} or faster at $w\to\infty$. This means that the Fermi function $f(w)$ in the definition of P can be replaced by $f(w)+\text{const}$. Another important case is when $G(w)$ is replaced by 1 in Eq. (A26). In this case the contribution of the semicircles does not vanish, and the integral (A26) gives $\Sigma(z)$.

An alternative to the fully self-consistent treatment investigated in this paper has been proposed in Ref. 5. There, the averages of the form $\langle d_\sigma^\dagger a_{m\sigma}\rangle$ were ignored, and those of the type $\langle a_{m\sigma}^\dagger a_{m'\sigma}\rangle$ were approximated by $\delta_{mm'}\langle a_{m\sigma}^\dagger a_{m\sigma}\rangle$. Namely, $\mathcal{H}_{\text{net-dot}}$ was put to zero in the calculation of the averages. Upon such an approximation, $P_\sigma(z)\simeq 0$, and

$$Q_\sigma(z)\simeq\int \mathrm{Im}\left[\frac{\Sigma_\sigma(\omega-i\eta)}{\pi}\right]\frac{f(\omega)}{z-\omega}d\omega, \tag{A27}$$

reproducing Eq. (8) of Ref. 5. Another approximation of Eqs. (A22) and (A23), originally due to Lacroix,[11] has been recently analyzed in the context of quantum dots in Ref. 18. In this approximation one assumes the dot Green function to vary smoothly enough over the integration regimes in Eqs. (A22) and (A23), so that it can be taken out of the integrals. This ansatz reduces Eq. (9) of the text to a quadratic form. These two approximate solutions are discussed in Secs. III and IV.

APPENDIX B: DERIVATION OF THE POLYNOMIAL FUNCTION R

As explained in Sec. IV, the function

$$\begin{aligned}R(z)\equiv\Phi_\sigma(z)\tilde{\Phi}_\sigma(z)-\mathrm{X}_\sigma(z)\tilde{\mathrm{X}}_\sigma(z)&=i(\Gamma_\sigma+\Gamma_{\bar\sigma})[z-\epsilon_0-i\Gamma_{\bar\sigma}-I_\sigma(z+\sigma h)]\left[\langle 1-n_{d\bar\sigma}\rangle-\frac{\Gamma_{\bar\sigma}}{\pi}\int d\omega\frac{f(\omega)G_{\bar\sigma}^-(\omega)}{z+\bar\sigma h-\omega}\right]\\&-i(\Gamma_\sigma+\Gamma_{\bar\sigma})[z-\epsilon_0+i\Gamma_\sigma-I_{\bar\sigma}(z+\bar\sigma h)]\left[\langle 1-n_{d\sigma}\rangle-\frac{\Gamma_\sigma}{\pi}\int d\omega\frac{f(\omega)G_\sigma^+(\omega)}{z+\sigma h-\omega}\right]-(\Gamma_\sigma+\Gamma_{\bar\sigma})^2\left[\langle 1-n_{d\bar\sigma}\rangle\langle 1-n_{d\sigma}\rangle\right.\\&\left.-\frac{\Gamma_{\bar\sigma}}{\pi}\int d\omega\frac{f(\omega)G_{\bar\sigma}^-(\omega)}{z+\bar\sigma h-\omega}\frac{\Gamma_\sigma}{\pi}\int d\omega\frac{f(\omega)G_\sigma^+(\omega)}{z+\sigma h-\omega}\right]\end{aligned} \tag{B1}$$

is nonsingular across the real axis, and its only singular point is at $z=\infty$. This observation enables one to solve for the Green function in terms of the functions Φ and $\tilde{\Phi}$. Here we examine $R(z)$ in some detail, and also derive the first two terms of its polynomial expansion.

In the limit $z\to\infty$, the function $I_\sigma(z)$, Eq. (31), is given by

$$I_\sigma(z)\sim\frac{\Gamma_\sigma}{\pi}\ln\frac{D_\sigma}{z}. \tag{B2}$$

The $z\to\infty$ limit of the integrals appearing in Eq. (B1) has to be taken with care. We write the Green functions appearing in the integrands there in the form $G_\sigma^\pm(\omega)=\mathrm{Re}\,G_\sigma^+(\omega)\pm i\,\mathrm{Im}\,G_\sigma^+(\omega)$, and use $\langle n_{d\sigma}\rangle=-(1/\pi)\times\int d\omega f(\omega)\mathrm{Im}\,G_\sigma^+(\omega)$ to obtain

$$\frac{\Gamma_\sigma}{\pi}\int d\omega\frac{f(\omega)G_\sigma^\pm(\omega)}{z-\omega}\sim\mp i\frac{\Gamma_\sigma\langle n_{d\sigma}\rangle}{z}+A_\sigma(z), \tag{B3}$$

where

$$A_\sigma(z)=\frac{\Gamma_\sigma}{\pi}\int d\omega\frac{f(\omega)\mathrm{Re}\,G_\sigma^+(\omega)}{z-\omega}. \tag{B4}$$

Inserting Eqs. (B2) and (B3) into Eq. (B1), the terms which survive the $z\to\infty$ limit are

$$\begin{aligned}R(z)\sim&(\Gamma_\sigma+\Gamma_{\bar\sigma})^2(\langle n_{d\sigma}\rangle+\langle n_{d\bar\sigma}\rangle-\langle n_{d\sigma}\rangle\langle n_{d\bar\sigma}\rangle)\\&+i(\Gamma_\sigma+\Gamma_{\bar\sigma})(z-\epsilon_0)\langle n_{d\sigma}-n_{d\bar\sigma}\rangle\\&+i(\Gamma_\sigma+\Gamma_{\bar\sigma})\left(z[A_\sigma(z)-A_{\bar\sigma}(z)]-\langle 1-n_{d\bar\sigma}\rangle\frac{\Gamma_\sigma}{\pi}\ln\frac{D_\sigma}{z}\right.\end{aligned}$$

$$+\langle 1-n_{d\sigma}\rangle\frac{\Gamma_{\bar\sigma}}{\pi}\ln\frac{D_{\bar\sigma}}{z}\Bigg). \tag{B5}$$

According to the discussion in Sec. IV, the terms logarithmic in z have to disappear. The integral giving $A_\sigma(z)$, Eq. (B4), is well behaved on the positive ω axis, since then for large ω the Fermi function makes it convergent. For very large negative ω values, $\mathrm{Re}\, G^+_\sigma(\omega)\to\langle 1-n_{d\bar\sigma}\rangle/\omega$, and as a result, the contribution from that part of the integration to $A_\sigma(z)$ is $\langle 1-n_{d\bar\sigma}\rangle(\Gamma_\sigma/\pi)(1/z)\ln(\zeta_\sigma/z)$, where $\zeta_\sigma\lesssim D_\sigma$. Hence, the terms logarithmic in z are canceled. In our calculations, we have used

$$A_\sigma(z)\sim-\frac{\Gamma_\sigma}{\pi}\langle 1-n_{d\bar\sigma}\rangle\ln\frac{z}{D_\sigma}+\frac{b_\sigma}{z}, \tag{B6}$$

and have determined the coefficient b_σ self-consistently (see Appendix C). In this way we find

$$R(z)=(\Gamma_\sigma+\Gamma_{\bar\sigma})^2[\langle n_{d\sigma}\rangle+\langle n_{d\bar\sigma}\rangle-\langle n_{d\sigma}\rangle\langle n_{d\bar\sigma}\rangle]+i(\Gamma_\sigma+\Gamma_{\bar\sigma})[(z-\epsilon_0)\langle n_{d\sigma}-n_{d\bar\sigma}\rangle+b_\sigma-b_{\bar\sigma}]. \tag{B7}$$

APPENDIX C: DETAILS OF THE EXACT SOLUTION

This appendix is devoted to the analysis of the exact solution for the self-consistent EOM, and in particular to the determination of the unknown coefficients b_σ [see Eqs. (B6) and (B7)], a and $\tilde a$ [see Eqs. (42)]. This is accomplished by expanding the solution at large frequencies, and equating the coefficients with those of the desired functions Φ and $\tilde\Phi$. We give the details for Φ; those of the "tilde" solution are obtained analogously.

As has been the case for the integral (B3), the large negative part of the integral defining $M_\sigma(z)$ has to be taken with care. To this end we write

$$M_\sigma(z)\equiv\int\left(-\frac{d\omega}{2\pi i}\right)\frac{\ln H_\sigma(\omega)}{z-\omega}=\int_{-\infty}^{+\infty}\left(-\frac{d\omega}{2\pi i}\right)\frac{\ln H_\sigma(\omega)-\Theta(-D_{\bar\sigma}-\omega)F_\sigma(\omega)(-2\pi i)}{z-\omega}+\int_{-\infty}^{-D_{\bar\sigma}}\frac{F_\sigma(\omega)d\omega}{z-\omega}, \tag{C1}$$

where the function $F_\sigma(\omega)$ is defined in such a way that the use of the geometric series $1/(z-\omega)=z^{-1}+z^{-2}\omega+\mathcal{O}(z^{-3})$ in the first integral of Eq. (C1) results in convergent integrals. It is sufficient to include in $F_\sigma(\omega)$ the most slowly decaying terms of $\ln H(\omega)/(-2\pi i)$, which are obtained by expanding $H(\omega)$ for large negative ω,

$$F_\sigma(\omega)=-\frac{\Gamma_{\bar\sigma}}{\pi\omega}-\frac{\Gamma_{\bar\sigma}}{\pi\omega^2}\left[\frac{\Gamma_{\bar\sigma}}{\pi}\ln\frac{D_{\bar\sigma}}{|\omega|}+\epsilon_0-i(\Gamma_\sigma+\Gamma_{\bar\sigma})\langle n_{d\sigma}\rangle+i\Gamma_{\bar\sigma}\right]. \tag{C2}$$

[In this expansion one has to include terms of the order $\mathcal{O}(\omega^{-2})$ because of the linear term in the prefactor in Eq. (42).] Using Eq. (C2), the second integral in Eq. (C1) is obtained explicitly, and then expanded up to order z^{-2},

$$\int_{-\infty}^{-D_{\bar\sigma}}\frac{F_\sigma(\omega)d\omega}{z-\omega}\sim\frac{\Gamma_{\bar\sigma}}{\pi z}\ln\frac{z}{D_{\bar\sigma}}-\frac{1}{2}\left(\frac{\Gamma_{\bar\sigma}}{\pi z}\ln\frac{z}{D_{\bar\sigma}}\right)^2+\frac{\Gamma_{\bar\sigma}^2}{\pi^2D_{\bar\sigma}z}-\frac{\Gamma_{\bar\sigma}^2}{6z^2}+\frac{D_{\bar\sigma}\Gamma_{\bar\sigma}}{\pi z^2}-\frac{\Gamma_{\bar\sigma}}{\pi}[\epsilon_0-i(\Gamma_\sigma+\Gamma_{\bar\sigma})\langle n_{d\sigma}\rangle+i\Gamma_{\bar\sigma}]\left[\frac{1}{zD_{\bar\sigma}}-\frac{1}{z^2}\ln\frac{z}{D_{\bar\sigma}}\right]. \tag{C3}$$

As a result, the asymptotic expansion of the function $M_\sigma(z)$ becomes

$$M_\sigma(z)\sim[\alpha_\sigma+(\Gamma_{\bar\sigma}/\pi)\ln(z/D_{\bar\sigma})]/z+\{\beta_\sigma+(\Gamma_{\bar\sigma}/\pi)[\epsilon_0-i(\Gamma_\sigma+\Gamma_{\bar\sigma})\langle n_{d\sigma}\rangle+i\Gamma_{\bar\sigma}]\ln(z/D_{\bar\sigma})-(\Gamma_{\bar\sigma}/\pi)^2(1/2)ln^2(z/D_{\bar\sigma})\}/z^2, \tag{C4}$$

where the coefficients α_σ and β_σ are given by

$$\alpha_\sigma=\frac{\Gamma_{\bar\sigma}^2}{\pi^2D_{\bar\sigma}}-\frac{\Gamma_{\bar\sigma}}{\pi D_{\bar\sigma}}[\epsilon_0-i(\Gamma_\sigma+\Gamma_{\bar\sigma})\langle n_{d\sigma}\rangle+i\Gamma_{\bar\sigma}]+\int_{-\infty}^{+\infty}[i\ln H_\sigma(\omega)/(2\pi)-\Theta(-D_{\bar\sigma}-\omega)F_\sigma(\omega)]d\omega, \tag{C5}$$

$$\beta_\sigma=-\frac{\Gamma_{\bar\sigma}^2}{6}+\frac{\Gamma_{\bar\sigma}D_{\bar\sigma}}{\pi}+\int_{-\infty}^{+\infty}\omega[i\ln H_\sigma(\omega)/(2\pi)-\Theta(-D_{\bar\sigma}-\omega)F_\sigma(\omega)]d\omega. \tag{C6}$$

An analogous calculation gives $\tilde F_\sigma(\omega)=F_{\bar\sigma}(\omega)^*$, leading to

$$\tilde{M}_\sigma(z) \sim [\tilde{\alpha}_\sigma + (\Gamma_\sigma/\pi)\ln(z/D_\sigma)]/z + \{\tilde{\beta}_\sigma + (\Gamma_\sigma/\pi)[\epsilon_0 + i(\Gamma_\sigma + \Gamma_{\bar{\sigma}})\langle n_{d\bar{\sigma}}\rangle - i\Gamma_\sigma] \times \ln(z/D_\sigma) - (\Gamma_\sigma/\pi)^2(1/2)\ln^2(z/D_\sigma)\}/z^2, \quad \text{(C7)}$$

$$\tilde{\alpha}_\sigma = \frac{\Gamma_\sigma^2}{\pi^2 D_\sigma} - \frac{\Gamma_\sigma}{\pi D_\sigma}[\epsilon_0 + i(\Gamma_\sigma + \Gamma_{\bar{\sigma}})\langle n_{d\bar{\sigma}}\rangle - i\Gamma_\sigma] + \int_{-\infty}^{+\infty}[i \ln \tilde{H}_\sigma(\omega)/(2\pi) - \Theta(-D_\sigma - \omega)\tilde{F}_\sigma(\omega)]d\omega, \quad \text{(C8)}$$

$$\tilde{\beta}_\sigma = -\frac{\Gamma_\sigma^2}{6} + \frac{\Gamma_\sigma D_\sigma}{\pi} + \int_{-\infty}^{+\infty}\omega[i \ln \tilde{H}_\sigma(\omega)/(2\pi) - \Theta(-D_\sigma - \omega)\tilde{F}_\sigma(\omega)]d\omega. \quad \text{(C9)}$$

Finally, we use Eqs. (C4) and (C7) in Eq. (42), and then compare term by term with the expansion of Eq. (33). This procedure determines the coefficients a and $\tilde{a}$,

$$a = \alpha_\sigma + \epsilon_0 - i\Gamma_\sigma, \quad \tilde{a} = \tilde{\alpha}_\sigma + \epsilon_0 + i\Gamma_{\bar{\sigma}}, \quad \text{(C10)}$$

and gives the self-consistency equations

$$b_{\bar{\sigma}} + i\Gamma_{\bar{\sigma}}\langle n_{d\bar{\sigma}}\rangle = i(\Gamma_\sigma + \Gamma_{\bar{\sigma}})^{-1}[\beta_\sigma - a\alpha_\sigma + \alpha_\sigma^2/2 + \Gamma_{\bar{\sigma}}h/(2\pi)], \quad \text{(C11)}$$

$$b_\sigma - i\Gamma_\sigma\langle n_{d\sigma}\rangle = -i(\Gamma_\sigma + \Gamma_{\bar{\sigma}})^{-1}[\tilde{\beta}_\sigma - \tilde{a}\tilde{\alpha}_\sigma + \tilde{\alpha}_\sigma^2/2 - \Gamma_\sigma h/(2\pi)]. \quad \text{(C12)}$$

In the case of a full spin symmetry (including $h=0$), one has $\tilde{\alpha}=\alpha^*$, $\tilde{\beta}=\beta^*$, and $\tilde{a}=a^*$, and then Eq. (C11) and Eq. (C12) become complex conjugate.

For a given set of parameters, Eqs. (C11) and (C12) are solved numerically for b_σ and $\langle n_{d\sigma}\rangle$ by an iterative Newton-Raphson algorithm. The initial values are chosen from the solution of the noninteracting ($U=0$) problem.

*Electronic address: slava@latnet.lv

[1] L. Kouwenhoven, C. Marcus, P. McEuen, S. Tarucha, R. Westervelt, and N. Wingreen, in *Mesoscopic Electron Transport*, edited by L. L. Sohn, L. P. Kouwenhoven, and G. Schön (Kluwer, Dordrecht, 1997).

[2] P. W. Anderson, Phys. Rev. **124**, 41 (1961).

[3] T. K. Ng and P. A. Lee, Phys. Rev. Lett. **61**, 1768 (1988); L. I. Glazman and M. E. Raĭkh, Pis'ma Zh. Eksp. Teor. Fiz. **47**, 378 (1988) [JETP Lett. **47**, 452 (1988)].

[4] A. C. Hewson, *The Kondo Problem to Heavy Fermions* (Cambridge University Press, Cambridge, England, 1993).

[5] Y. Meir, N. S. Wingreen, and P. A. Lee, Phys. Rev. Lett. **66**, 3048 (1991).

[6] J. E. Hirsch and R. M. Fye, Phys. Rev. Lett. **56**, 2521 (1986); R. N. Silver, J. E. Gubernatis, D. S. Sivia, and M. Jarrell, *ibid.* **65**, 496 (1990).

[7] K. G. Wilson, Rev. Mod. Phys. **47**, 773 (1975); T. A. Costi, A. C. Hewson, and V. Zlatić, J. Phys.: Condens. Matter **6**, 2519 (1994); W. Hofstetter, Phys. Rev. Lett. **85**, 1508 (2000).

[8] D. N. Zubarev, Usp. Fiz. Nauk **71**, 71 (1960) [Sov. Phys. Usp. **3**, 320 (1960)].

[9] A. Theumann, Phys. Rev. **178**, 978 (1969).

[10] (a) J. A. Appelbaum and D. R. Penn, Phys. Rev. **188**, 874 (1969); (b) Phys. Rev. B **3**, 942 (1971).

[11] C. Lacroix, J. Phys. F: Met. Phys. **11**, 2389 (1981).

[12] C. Lacroix, J. Appl. Phys. **53**, 2131 (1982).

[13] H. Mamada and F. Takano, Prog. Theor. Phys. **43**, 1458 (1970).

[14] G. S. Poo, Phys. Rev. B **11**, 4606 (1975); **11**, 4614 (1975).

[15] T. K. Ng, Phys. Rev. Lett. **76**, 487 (1996).

[16] R. Fazio and R. Raimondi, Phys. Rev. Lett. **80**, 2913 (1998); Q. F. Sun, H. Guo, and T. H. Lin, *ibid.* **87**, 176601 (2001).

[17] P. Zhang, Q.-K. Xue, Y. P. Wang, and X. C. Xie, Phys. Rev. Lett. **89**, 286803 (2002); N. Sergueev, Q. F. Sun, H. Guo, B. G. Wang, and J. Wang, Phys. Rev. B **65**, 165303 (2002).

[18] O. Entin-Wohlman, A. Aharony, and Y. Meir, Phys. Rev. B **71**, 035333 (2005).

[19] B. R. Bułka and P. Stefanski, Phys. Rev. Lett. **86**, 5128 (2001).

[20] H.-G. Luo, S.-J. Wang, and C.-L. Jia, Phys. Rev. B **66**, 235311 (2002).

[21] B. R. Bułka and S. Lipiński, Phys. Rev. B **67**, 024404 (2003).

[22] E. C. Goldberg, F. Flores, and R. C. Monreal, Phys. Rev. B **71**, 035112 (2005).

[23] R. C. Monreal and F. Flores, Phys. Rev. B **72**, 195105 (2005).

[24] N. Sivan and N. S. Wingreen, Phys. Rev. B **54**, 11622 (1996).

[25] J. König and Y. Gefen, Phys. Rev. B **71**, 201308(R) (2005).

[26] See footnote 8 in Ref. 9.

[27] H.-G. Luo, J.-J. Ying, and S.-J. Wang, Phys. Rev. B **59**, 9710 (1999).

[28] Keeping the EOM of these Green functions and decoupling the resulting higher-order EOM has been proposed in Ref. 27 as a possible way to improve the present approximation. We have tried to investigate this proposal but could not reproduce the results of that paper. Instead, we have found that the scheme becomes untractable.

[29] L. Dworin, Phys. Rev. **164**, 818 (1967); **164**, 841 (1967).

[30] A. Oguchi, Prog. Theor. Phys. **43**, 257 (1970).

[31] D. C. Langreth, Phys. Rev. **150**, 516 (1966).

[32] In fact, in order to obtain the result (31) it suffices to make the assumption (27) only over an energy scale which is much smaller than the bandwidth, say $[-D_\sigma^{\rm low}; D_\sigma^{\rm up}]$. Possible energy dependencies of the self-energy on larger scales can then be incorporated into D_σ, by normalizing the lower cutoff on the band, $D_\sigma \equiv D_\sigma^{\rm low} \exp \int_{-D_\sigma^{\rm low}}^{0}[1 - {\rm Im}\,\Sigma_\sigma^-(\omega)/\Gamma_\sigma]/\omega\, d\omega$. This may be necessary when the dot is embedded in a complex mesoscopic network.

[33] P. E. Bloomfield and D. R. Hamann, Phys. Rev. **164**, 856 (1967).

[34] N. I. Muskhelishvili, *Singular Integral Equations*, 2nd ed. (Do-

ver, New York, 1992).

[35] In such a case the so-called index of the Riemann-Hilbert problem (Ref. 34) is zero. If the integration limits in Eq. (42) are to be kept finite, one has to assume $D \equiv D_\sigma$ and possibly consider additional multiplicative powers of $(z \pm D)$, see Ref. 33. We ignore these options since they only affect the corrections of order ω/D_σ.

[36] P. B. Wiegmann and A. M. Tsvelick, J. Phys. C **16**, 2281 (1983); E. Ogievetski, A. M. Tsvelick, and P. B. Wiegmann, *ibid.* **16**, L797 (1983).

[37] F. D. M. Haldane, Phys. Rev. Lett. **40**, 416 (1978); **40**, 911 (1978).

[38] Certain examples of the Friedel sum-rule violation by self-consistent EOM schemes have been discussed recently in Refs. 22 and 23.

[39] S. Kirchner, J. Kroha, and P. Wölfle, Phys. Rev. B **70**, 165102 (2004).

[40] P. Simon, O. Entin-Wohlman, and A. Aharony, Phys. Rev. B **72**, 245313 (2005).